



A Journal of the Gesellschaft Deutscher Chemiker

# Angewandte Chemie

GDCh

International Edition

www.angewandte.org

## Accepted Article

**Title:** Highly ordered quantum dot supramolecular assembly exhibiting photoinduced emission enhancement

**Authors:** Mitsuaki Yamauchi, Seiya Yamamoto, and Sadahiro Masuo

This manuscript has been accepted after peer review and appears as an Accepted Article online prior to editing, proofing, and formal publication of the final Version of Record (VoR). This work is currently citable by using the Digital Object Identifier (DOI) given below. The VoR will be published online in Early View as soon as possible and may be different to this Accepted Article as a result of editing. Readers should obtain the VoR from the journal website shown below when it is published to ensure accuracy of information. The authors are responsible for the content of this Accepted Article.

**To be cited as:** *Angew. Chem. Int. Ed.* 10.1002/anie.202015535

**Link to VoR:** <https://doi.org/10.1002/anie.202015535>

# Highly ordered quantum dot supramolecular assembly exhibiting photoinduced emission enhancement

Mitsuaki Yamauchi,<sup>\*[a]</sup> Seiya Yamamoto,<sup>[a]</sup> and Sadahiro Masuo<sup>\*[a]</sup>

[a] Dr. M. Yamauchi, S. Yamamoto, Prof. Dr. S. Masuo  
Department of Applied Chemistry for Environment  
Kwansei Gakuin University  
2-1 Gakuen, Sanda, Hyogo 669-1337 (Japan)  
E-mail: yamauchi@kwansei.ac.jp  
masuo@kwansei.ac.jp

Supporting information for this article is given via a link at the end of the document.

**Abstract:** Multicomponent supramolecular assembly systems enable the generation of materials with outstanding properties, not obtained from single-component systems, via a synergetic effect. Herein, we demonstrate a novel supramolecular coassembly system rendering highly ordered quantum dot (QD) arrangement structures formed via the self-assembly of azobenzene derivatives, where the photocontrollable photoluminescence (PL) properties of the QDs are realized based on photoisomerization. Upon mixing the assembled azobenzene derivatives and QDs in apolar media, a time-evolution coaggregation into hierarchical nanosheets with a highly ordered QD arrangement structure occurs. Upon photoirradiation, the nanosheets transform into ill-defined aggregates without arranged QDs together with enhancing the PL intensity. In days, the photoirradiated coaggregates undergo recovery of the PL properties corresponding to the arranged QDs through thermal isomerization.

## Introduction

In biological systems, multiple biomolecules and their nanostructures with individual functions self-organize into a multicomponent sophisticated assembly, such as a cell, leading to the generation of desirable and essential functions depending on the external environment under dynamic conditions.<sup>[1] [2] [3]</sup> Inspired by these systems, scientists have attempted the construction of supramolecular assemblies consisting of several different materials through social (integrative) self-sorting<sup>[4] [5] [6] [7] [8] [9] [10]</sup> to realize the high-performance and unexpected physical properties that are not obtained from single materials. As functional nanomaterials, colloidal semiconductor

nanocrystals, referred to as quantum dots (QDs), have attracted much attention because of their outstanding photoluminescence (PL) properties, such as a high photodurability, sharp PL spectra and tunable energy band gap depending on the QD size.<sup>[11] [12] [13]</sup> Due to the high dispersibility of QDs, most studies using QDs have been focused on the photophysical properties under single conditions, such as dispersed QDs in solution<sup>[14] [15]</sup> and single QD levels<sup>[16] [17] [18] [19]</sup>. On the other hand, understanding the physical properties derived from inter-QD interactions observed in the solid condition of QDs is quite important for the development of QD-based materials science.<sup>[20] [21] [22] [23]</sup> Although QD structures could be formed on substrates by the evaporation of solvents, such an assembly method gives rise to the formation of inhomogeneous and ill-defined structures, and furthermore, the formation of assembled QDs in solution is quite difficult.<sup>[24]</sup> Recently, we proposed a strategy to form assembled QDs assisted by the self-assembly of organic dyes.<sup>[25]</sup> However, the assemblies of QDs are still far from existing molecular assemblies that can form hierarchical nanostructures and exhibit smart functions, such as stimuli-responsivity.

Herein, we report a unique supramolecular QD assembly system exhibiting the formation of highly ordered QD arrangement structures and photocontrollable PL properties based on the isomerization of azobenzene (Figure 1). In this system, we utilize a self-assembling azobenzene derivative with an adhesion moiety onto the QD surface to realize photoresponsivity. Upon mixing the QDs and assembled azobenzene derivatives in apolar media, the mixture undergoes a time-evolution coassembly due to the adhesion of the QDs to the azobenzene assemblies.

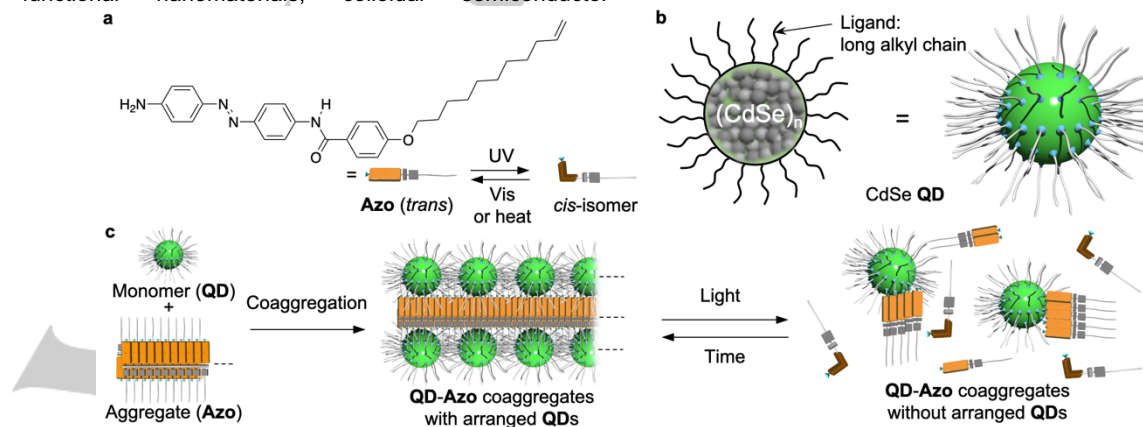


**Figure 1.** (a) Molecular structure of **Azo**. The inset shows the *trans*-to-*cis* isomerization of **Azo**. (b) Chemical structure of **QDs**. (c) Schematic illustration of the coaggregation of monomeric **QDs** and **Azo** aggregates into coaggregates with arranged **QDs** and their photoirradiation-induced transformation and time-dependent recovery behaviours.

An in-depth microscopic analysis of the resultant coassemblies reveals the formation of hierarchical nanosheets with a highly ordered QD arrangement structure. In the nanosheets, an energy transfer between neighbouring QDs was observed. Upon photoirradiation, the nanosheets transformed into ill-defined aggregates that showed a lower efficiency of energy transfer. Furthermore, the photoirradiated coaggregates underwent recovery of the PL properties corresponding to the arranged QDs through thermal isomerization. Our strategy for creating functional QD materials using molecular assembly can contribute to the development of nanoparticle-based materials science.

## Results and Discussion

### Molecular design

To realize the self-assembly, the adhesion to QDs and the photoresponse, we designed and synthesized a *trans*-azobenzene derivative (referred to as **Azo**, Figure 1a). The compound possesses an amide group for hydrogen bonding, an amino group for adhesion onto QDs and an azobenzene moiety for photoisomerization<sup>[26] [27]</sup>. The synthetic method of **Azo** and the characterization using <sup>1</sup>H and <sup>13</sup>C nuclear magnetic resonance (NMR) spectroscopies and electrospray ionization (ESI) mass spectrometry are described in the Supporting Information (Figure S1,2). As a QD, a well-studied CdSe quantum dot (referred to as **QD**), capped with surface protecting ligands of long alkyl chains, such as hexadecylamine, was synthesized according to the reported method with minor modifications (Figure 1b, see Supporting Information). The ultraviolet/visible (UV/vis) absorption spectrum of a diluted CHCl<sub>3</sub> solution of the **QD** ([**QD**] = 0.5 μM) showed a first peak at 519 nm (Figure S3a), by which the diameter of the **QD** without ligands was estimated to be ca. 2.7 nm.<sup>[28]</sup> The size is consistent with transmission electron microscopy (TEM) analysis of the **QD** (2.6 ± 0.1 nm, Figure S3b,c). The PL spectrum under 405 nm excitation showed a maximum wavelength at 527 nm with a narrow full width at half maximum (FWHM) of 28 nm (Figure S3a).

### Self-assembly of Azo

Generally, in a good solvent (CHCl<sub>3</sub>), noncovalent interactions such as hydrogen bonding are unfavourable, while in a poor solvent (cyclohexane), the interactions can be favourable.<sup>[29] [30]</sup> Before mixing **Azo** with **QDs**, we investigated the self-aggregation behaviors of sole **Azo** ([**Azo**] = 50 μM) in a poor solvent (cyclohexane:CHCl<sub>3</sub> = 9:1, v/v). As the **Azo** was not soluble in cyclohexane, the solution of **Azo** aggregates was prepared by adding cyclohexane into the **Azo** solution in CHCl<sub>3</sub>. The temperature-dependent absorption spectra from 55 to 20 °C showed a slight redshift with increasing absorbance, suggesting the planarization of azobenzene moieties and/or the formation of weak π–π stacking between azobenzene moieties (Figure S4a). Furthermore, the spectra at 20 °C did not change in the concentration range of 5–300 μM, indicating the assembly maintains at least at 5 μM (Figure S4b). The Fourier transform infrared (FTIR) spectroscopic measurements of the concentrated solution of **Azo** aggregates indicate the formation of a hydrogen-bond between amide groups and no hydrogen-bond between amino groups (Figure S4c). The atomic force

microscopy (AFM) analysis of the aggregates revealed the formation of short fibrous nanostructures with hundreds of nanometers in length (Figure 2a, S4d). The AFM cross-sectional analysis indicates that the heights of the lowest fibrous nanostructures are 5 nm (Figure 2b) and those of others exceed 5 nm. The heights are larger than that of a monolayer of hydrogen-bonded **Azo** (< 1 nm). Therefore, the fibrous nanostructures (two-dimensional (2D) aggregates) are formed by stacking of the hydrogen-bonded one-dimensional (1D) **Azo** aggregates (Figure 2c). This 2D nanostructure is expected to be formed based on a macrodipole moment<sup>[31]</sup> (Figure 2c). The macrodipole moment can be formed by a parallel arrangement of the weak dipole moment of **Azo**. Hence, the observed 2D aggregates may be formed by an antiparallel stacking of the 1D aggregates (Figure 2c). The TEM images also showed the formation of multilayer structures of **Azo** aggregates (Figure S4e). The resulting 2D aggregate is referred to as **Agg**<sub>Azo</sub>.

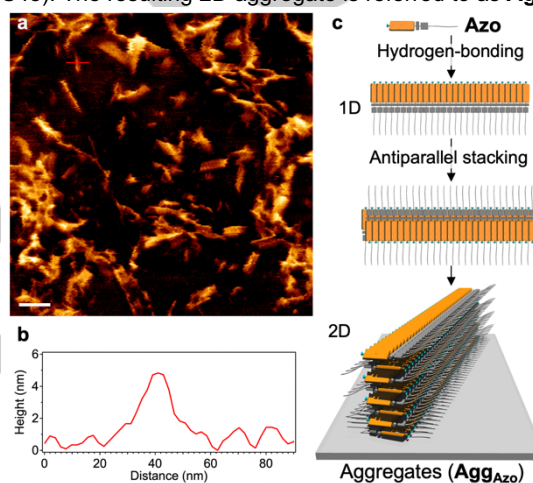


**Figure 2.** (a) AFM image of **Agg**<sub>Azo</sub> obtained from the solution of **Azo** aggregates ([**Azo**] = 50 μM). The scale bar is 100 nm. (b) The cross section along the red line in (a). (c) Schematic illustration of the possible 2D self-assembly of **Azo**.

### The formation of QD-Azo coaggregates

To confirm the adhesion of **Azo** onto **QDs**, we measured <sup>1</sup>H NMR spectra in [D<sub>8</sub>]toluene. The spectrum of sole **Azo** solution ([**Azo**] = 1 mM) showed a sharp proton signal of the amino group, indicating that the amino group is not bound to another **Azo** (Figure S5). Upon mixing the **Azo** and the **QD** ([**QD**]:[**Azo**] = 1:100, [**Azo**] = 1 mM), the signal of the amino group underwent a downfield shift with a signal broadening (Figure S5). This change indicates the adhesion of amino group of **Azo** onto the **QD** surface in toluene.

In order to form highly ordered **QD-Azo** coaggregates in solution, we mixed the solution of **Agg**<sub>Azo</sub> in cyclohexane:CHCl<sub>3</sub> (9:1, v/v) and a dry film of **QDs**. This film can easily be dispersed to monomeric **QDs** by adding the solution. Therefore, the mixing method can lead to the coaggregation of monomeric **QDs** and **Agg**<sub>Azo</sub>. The ratio of **QDs** and **Azo** was 1:100 ([**QD**] = 0.5 μM, [**Azo**] = 50 μM) to facilitate extended aggregation and thereby suppress the formation of small aggregates, such as **QD-Azo** dimers.<sup>[25] [32]</sup> The coaggregation behaviours were investigated by PL spectra and PL decay curves. Upon mixing the **QDs** and **Agg**<sub>Azo</sub>, the PL intensity at 527 nm decreased by half (*t* = 0 min) and thereafter decreased gradually over 180 min (Figure. 3a). The analysis of the decay curves revealed a clear decrease in the average lifetime (*τ*<sub>ave</sub>) to 11.2 ns (*t* = 0

min) and 4.0 ns ( $t = 180$  min) compared to that of only QDs (21.4 ns, Figure. 3b, Table S1). These results indicate the formation of coaggregates of QDs and  $\text{Agg}_{\text{Azo}}$ . In contrast, the absorption spectra did not show a time-dependent change (Figure 3c), suggesting that electronic coupling between the QDs in the ground state did not occur. Furthermore, we investigated the effect of the adhesion of amino groups to QDs on the PL behaviors. As a result, the addition of oleylamine induced the PL increase, indicating that the adhesion of amino groups did not induce the PL decrease (Figure S3d,e). Therefore, the PL decrease is attributed to QD–QD and/or QD–Azo interactions at the excited state, such as the excitation energy transfer. As there is spectral overlap between the PL spectrum of the QDs and the absorption spectra of the QDs and Azo, energy transfer can occur in the QD–Azo coaggregates (Figure S6). Considering the relationship between the energy levels of the molecular orbitals of Azo and bands of QDs,<sup>[35]</sup> the possibility of electron transfer between the excited QDs and Azo is excluded (Figure S7). The PL quenching of QDs by energy transfer can be explained by the following reasons. For the PL quenching by energy transfer to Azo, this is because the energy acceptor (Azo) is nonemissive.<sup>[33]</sup> For the PL quenching by energy transfer between QDs, it can be explained as follows. The emission quantum yield of our QD is not unity, indicating that the excitons decay nonradiatively by trapping at defect sites in the QD. This trapping rate is faster than that of energy transfer to next QD. Therefore, the energy transferred to the next QD is further trapped at defect sites in the next QD. Hence, the multiple occurrence of energy transfers between QDs, which is known as exciton diffusion<sup>[21]</sup> [34], can lead to the PL quenching. Based on the above discussion, the time change in PL behaviours corresponds to the occurrence of energy transfer between the QD–QD and from the QD to Azo upon coaggregation. This detailed mechanism is discussed in a later section.

Dynamic light scattering (DLS) measurements were carried out to evaluate the aggregate size in solution (Figure 3d, Figure S8). For the  $\text{Agg}_{\text{Azo}}$  ( $[\text{Azo}] = 50 \mu\text{M}$ ), aggregates with a hydrodynamic diameter ( $D_h$ ) of approximately 100 nm were detected. The size is consistent with the length of short nanofibers obtained from AFM (Figure S2a). For the sole QDs,

a  $D_h$  of approximately 7 nm was detected, which is similar to the diameter of QDs containing ligands (5–6 nm, Figure S3c). Upon mixing the  $\text{Agg}_{\text{Azo}}$  with QDs, the resulting coaggregates of the QDs and Azo (referred to as  $\text{Agg}_{\text{QD-Azo}}$ ) showed a larger  $D_h$  of approximately 300 nm ( $t = 0$  min) together with free monomeric QDs and/or Azo-adsorbed QDs in which small  $\text{Agg}_{\text{Azo}}$  adsorbed on QDs (Figure 3d). Given that the size of  $\text{Agg}_{\text{Azo}}$  did not increase over time, the increased size of  $\text{Agg}_{\text{QD-Azo}}$  by adding QDs is presumably due to the adsorption of QDs to multiple  $\text{Agg}_{\text{Azo}}$ , in which a QD acts as a linker between the  $\text{Agg}_{\text{Azo}}$ . The  $D_h$  did not show the time-dependent growth at  $t = 60, 180$  min. These results indicate that the larger  $\text{Agg}_{\text{QD-Azo}}$  was formed even just after mixing and the size did not change with time. Taking the time-dependent PL decrease into account, the PL time-change is presumably due to increasing energy transfer between QDs by a further adhesion of free QDs to the  $\text{Agg}_{\text{QD-Azo}}$  over time. (For details, see “Coaggregation mechanism” section).

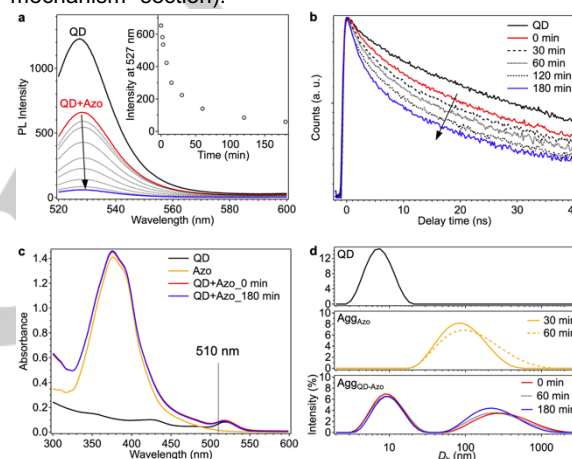


**Figure 3.** (a,b) Time-dependent PL spectra (a) and PL decay curves (b) of the QD–Azo mixture (QD:Azo = 1:100, [QD] = 0.5  $\mu\text{M}$ ) in cyclohexane/ $\text{CHCl}_3$  (9:1, v/v) after mixing QD and Azo ( $\lambda_{\text{ex}} = 510$  nm, at which QD has large absorption, while Azo has subtle absorption). The data of only QDs ([QD] = 0.5  $\mu\text{M}$ ) are shown as comparison. The inset in (a) shows the plot of the PL intensity as a function of time. (c) Absorption spectra of the QDs ([QD] = 0.5  $\mu\text{M}$ ), Azo ([Azo] = 50  $\mu\text{M}$ ), and their mixture at  $t = 0, 180$  min (QD:Azo = 1:100, [QD] = 0.5  $\mu\text{M}$ ) in cyclohexane/ $\text{CHCl}_3$  (9:1, v/v). (d) DLS-derived size distribution of the hydrodynamic diameter ( $D_h$ ) of QDs,  $\text{Agg}_{\text{Azo}}$  and  $\text{Agg}_{\text{QD-Azo}}$  formed in cyclohexane/ $\text{CHCl}_3$  (9:1, v/v).

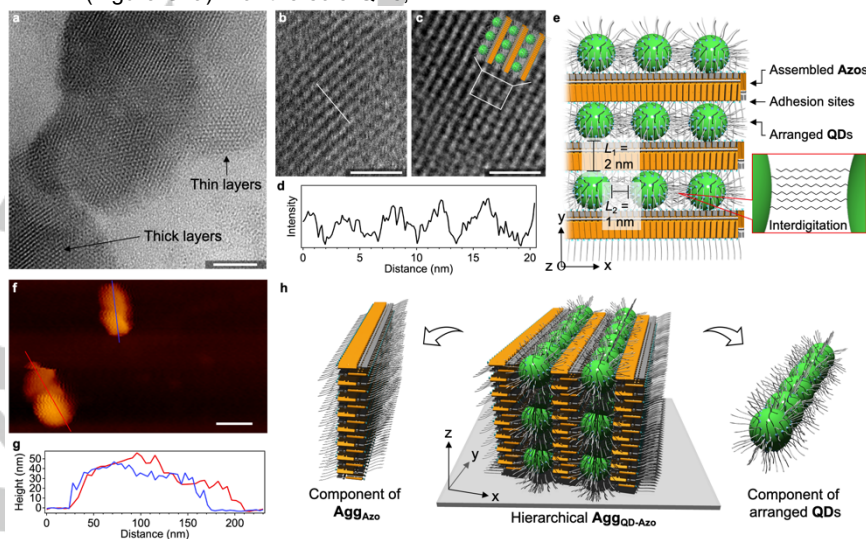


**Figure 4.** (a–c) TEM image (a) and magnified TEM images (b,c) of the stripe-like coaggregates ( $\text{Agg}_{\text{QD-Azo}}$ ) with the corresponding cartoon image. Scale bars in (a) and (b,c) are 50 nm and 20 nm, respectively. (d) The cross section along the white line in (b). (e) Schematic illustration of the nanostructure of  $\text{Agg}_{\text{QD-Azo}}$ . (f) AFM image of  $\text{Agg}_{\text{QD-Azo}}$ . The scale bar is 100 nm. (g) The cross-sectional analysis along the lines in (f). (h) Schematic illustration of possible hierarchical coaggregation composed of 2D  $\text{Agg}_{\text{Azo}}$  and arranged QDs.

### The nanostructure of highly ordered QD-Azo coaggregates

To visualize the morphology of **Agg<sub>QD-Azo</sub>**, we performed TEM and AFM of samples spin-coated from the solution. The TEM images allow us to find a stripe-like two-dimensional (2D) nanosheet (Figure 4a–d, S9), in which a black line width within the stripe was approximately 2.5 nm (Figure 4c), which is consistent with the diameter of the **QDs** without ligands (2.6 nm) (Figure S3b,c). Such stripe formation means a 2D arrangement of the **QDs** with high electron density. Furthermore, the cross-sectional analysis (Figure 4d) revealed that the edge-to-edge length between one-dimensionally arranged **QDs** ( $L_1$ ) is approximately 2 nm (Figure 4e), which is consistent with the length of the rigid aromatic moieties of **Azo** (1.8 nm). We confirmed that such a unique nanosheet could not be formed by using sole **QDs** and **Azo** (Figure S3b, S4d). Accordingly, the nanosheet with a highly ordered **QD** arrangement structure is formed along the assembled **Agg<sub>Azo</sub>**, as illustrated in Figure 4(e). For the 2D arrangements, the **Agg<sub>Azo</sub>** should have the two adsorption sites composed of amino groups on both sides. Considering the self-assembly behaviors of **Azo**, the **Agg<sub>Azo</sub>** in the coaggregates are also expected to form hydrogen bonding between amide groups and undergo the antiparallel stack between the fibrous aggregates (Figure 2b). Therefore, the **Agg<sub>Azo</sub>** with the two adsorption sites contributes to the formation of nanosheets composed of arranged **QDs** and **Agg<sub>Azo</sub>**. In addition, TEM analysis showed that the edge-to-edge length between **QDs** ( $L_2$ ) was approximately 1 nm at the closest position (Figure 4e), and it was found that this close distance between the **QDs** enables energy transfer between neighbouring **QDs**. Additionally, the  $L_2$  was twice as small as the average length between the **QDs** (2 nm), obtained from the **QD** solution by natural drying (Figure S3c). This result indicates that an interdigitation between the ligands of **QDs** occurs in the nanosheet, as shown in Figure 4(e). Therefore, the van der Waals force between ligands for interdigitation plays an important role in facilitating the formation of **QD** arrangements. Considering that the coaggregation showed time dependent PL properties, monomeric **QDs** and **Agg<sub>Azo</sub>** was integrated into complex coaggregates (**Agg<sub>QD-Azo</sub>**) through time-dependent social self-sorting.

Notably, we found that the different contrasts in the TEM image (Figure 4a), where grey and black areas coexist and the latter means thick coaggregates, indicates the formation of 3D multilayer nanostructures. The magnified images of the thin and thick layers are shown in Figures (4b, 4c), respectively. Comparing the two layers, the arranged **QDs** (black stripes) at the thick layer (Figure 4c) are clearly identified with the high contrast to the thin layer (Figure 4b). This high contrast indicates that the lower layers also have **QD** arrangement structures similar to that of the top layer, as shown in Figure 4(h). Furthermore, the AFM image revealed that the coaggregates have the areas of different heights (10–50 nm) (Figure 4f,g). As the **QD** size containing ligands is 5–6 nm, the thick coaggregates are expected to have a hierarchical multilayer structure (Figure 4h). Based on the self-assembly behaviors of **Azo**, the hierarchical 3D structure of **Agg<sub>QD-Azo</sub>** may contain the 2D aggregates of **Agg<sub>Azo</sub>**, formed by a successive antiparallel stacking of single hydrogen-bonded aggregates of **Azo**, and arranged **QDs** (Figure 4h). Therefore, the driving force for the formation 3D multilayers would be the adhesion of **QDs** to both sides of 2D **Agg<sub>Azo</sub>**, in which this

adhesion can be stabilized by van der Waals force between alkyl chains (ligands) on the **QD** and between the ligand and alkyl chain of **Azo**. Accordingly, we created a novel highly ordered nanostructure with semiconductor nanocrystals and organic molecules.

### Coaggregation mechanism

To obtain insight into the coaggregation mechanism, we focused on the time-dependent PL decrease caused by energy transfers from the **QDs** to **Azo** and **QDs**. Assuming **Azo** acts as a PL quencher, we investigated the PL spectra of **Agg<sub>QD-Azo</sub>** upon changing the concentration of **Azo** ( $[QD] = 0.5 \mu\text{M}$ , **QD:Azo** = 1:0, 10, 20, 60, 100). As a result, a time decrease in the PL intensity for several hours was observed at all ratios except for the pure **QD** solution (Figure S10). When the PL intensity ratio ( $I_{QD}/I_{QD-Azo}$ ) was plotted against the concentration of **Azo** ( $[Azo]$ ) at  $t = 0, 60, 120, 180$  min, the plot at  $t = 0$  min showed a linear relationship, that is, a Stern–Volmer plot with only one type of quenching (Figure 5a). The results indicate that the PL quenching of **QDs** observed under just mixed conditions ( $t = 0$  min) is stoichiometrically caused by the energy transfer from **QDs** to **Azo**. Based on the results, we could expect that at  $t = 0$  min, the adhesion of **QDs** to **Agg<sub>Azo</sub>** predominately occurs in comparison with the arrangement of **QDs**. The fitting with the Stern–Volmer equation<sup>[36]</sup> ( $I_{QD}/I_{QD-Azo} = 1 + k_q \tau_{QD}[Azo]$ ) afforded a quenching rate constant ( $k_q$ ) of  $2.9 \times 10^{12} \text{ M}^{-1} \text{ s}^{-1}$ . This value is much higher than that obtained in a typical diffusion system of donor and acceptor molecules ( $k_q < 10^{10} \text{ M}^{-1} \text{ s}^{-1}$ ),<sup>[36]</sup> which indicates that **QDs** chemically adsorbs to the **Agg<sub>Azo</sub>**. In contrast, the plots at the later stage after mixing ( $t = 60, 120, 180$  min) deviate from the linear relationship and appear to be a logarithmic curve (Figure 5a). This trend is probably due to a saturation of the energy transfer upon concentrating **Azo**. Such deviation has not been observed in the simple adhesion system of merocyanine dyes to CdSe/ZnS **QDs** at similar concentration ratios.<sup>[37]</sup> Considering the close distance between the **QDs** in the **Agg<sub>QD-Azo</sub>**, as revealed by TEM, the energy transfer (energy hopping) between **QD–QD** can be accelerated over time. Based on the discussion, we could conclude that the coaggregation process is involved with an adhesion step of the **QD** to **Agg<sub>Azo</sub>** at  $t = 0$  min, where energy transfer between **QD–Azo** occurs predominately. Furthermore, at  $t = 60–180$  min, a further adhesion of free **QDs** to **Agg<sub>Azo</sub>** with **QDs** is expected to occur (Figure 5b). The adhesion can lead to arrangements of **QDs** on **Agg<sub>Azo</sub>**, where energy transfer between **QD–QD** occurs in addition to that from the **QD** to **Azo**.

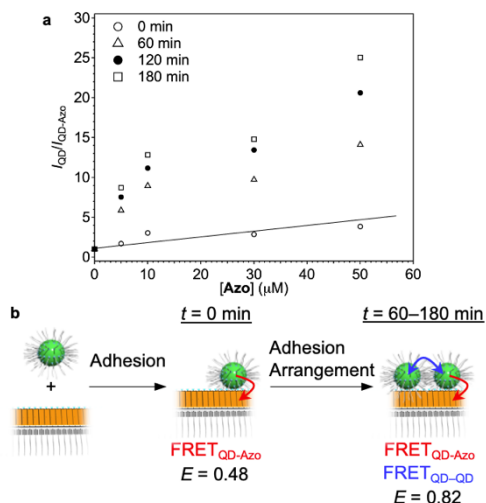


**Figure 5.** (a) Plots of  $I_{QD}/I_{QD-Azo}$  against the concentration of **Azo** ( $[Azo]$ ) at  $t = 0, 60, 120, 180$  min. The line corresponds to the Stern–Volmer plot ( $I_{QD}/I_{QD-Azo} = 1 + k_q \tau_{QD}[Azo]$ ). (b) A possible mechanism for the time-dependent coaggregation estimated from the in-depth analysis of the energy transfer.

Next, we compared the experimental and theoretical results of the energy transfer efficiency ( $E$ ) to reveal the in-depth coaggregation mechanism. Although the energy transfer mechanism involving **QDs** is generally explained by dipole–dipole coupling-based Förster-type resonance energy transfer (FRET) and electron exchange-based Dexter-type energy transfer<sup>[38]</sup>, the former mechanism is suitable for observed energy transfer (details in Supporting Information). To theoretically evaluate FRET, we used the spectral overlap between the PL spectrum of the **QDs** (donor) and the absorption spectrum of **Azo** (acceptor) or **QDs** (acceptor) (Figure S7) and found that the Förster distances ( $R_0$ ) of **QD-Azo** and **QD-QD**, at which  $E = 0.5$ , are estimated to be 1.4 and 4.3 nm, respectively. When the dipole–dipole distance ( $R$ ) is estimated from the **QD** centre to the **Azo** centre (2.0 nm) and **QD** centre (3.6 nm),<sup>[33]</sup> the  $E$  values of **QD-Azo** ( $E_{QD-Azo}$ ) and **QD-QD** ( $E_{QD-QD}$ ) are estimated to be 0.09 and 0.74, respectively. This estimation clearly indicates that the  $E_{QD-Azo}$  value is lower than the  $E_{QD-QD}$  value. To evaluate the observed FRET in the coaggregates, we estimated the  $E$  value from the PL lifetimes ( $\tau$ ). Although the  $E$  value of FRET can be calculated with either the PL intensity or lifetime, we selected the  $\tau$  values for the exact valuation because the reabsorption of **QD** emission can affect the  $I_{QD-Azo}$  values. Using the equation  $E = 1 - \tau_{QD-Azo}/\tau_{QD}$ , the  $E$  values of **Agg<sub>QD-Azo</sub>** ( $t = 0$  and 180 min) are estimated to be 0.48 and 0.82, respectively (Table S1).

Considering the theoretically estimated  $E_{QD-Azo}$  (0.09), approximately ten **Azo** molecules are expected to adsorb onto the **QD** at  $t = 0$  min.<sup>[39]</sup> Over time, a more efficient FRET between **QD-QD** was facilitated (Figure. 5b). To confirm the FRET between **QD-QD**, we measured the PL decay curves of aggregated **QD** films, in which only **QD-QD** interactions can occur, on a glass substrate (Figure S11). Hence, the average lifetime was 6.6 ns, by which  $E_{QD-QD}$  is estimated to be 0.74. This  $E_{QD-QD}$  value is lower than  $E$  at  $t = 180$  min (0.82), which is because the distance between **QD-QD** in **Agg<sub>QD-Azo</sub>** is relatively shorter than that in the **QD** films.

### Photocontrol of coaggregates

The photoisomerization of azobenzene molecules should affect the assembled structures and the physical properties.<sup>[40]</sup> When the **Agg<sub>QD-Azo</sub>** solution was irradiated with a 365 nm UV lamp for 15 s to reach the photostationary state (PSS), the absorption band at 376 nm corresponding to the *trans*-azobenzene moiety decreased with increasing bands at approximately 470 nm corresponding to the *cis*-azobenzene moiety (Figure 6a). The *trans*:*cis* ratio is approximately 30:70 based on the spectral change. Upon irradiation with a 470 nm visible lamp for 90 s to reach the PSS, back-isomerization from *cis*- to *trans*-isomer occurred (*trans*:*cis* = 70:30). With the same irradiation times, we conducted UV- and visible (Vis)-irradiation cycles multiple times and found efficient photoisomerization of **Azo** even in the coaggregates. Notably, this repetitious irradiation induced a PL increase in the **QDs** at 525 nm (Figure 6b). The PL decay curves showed an increase in  $\tau_{ave}$  from 4.6 to 7.7 ns (10 cycles of UV-Vis irradiation), by which the  $E$  value decreased from 0.79 to 0.64 (Figure S12a, Table S2). These results indicate that the contribution of FRET<sub>QD-QD</sub> decreased by photoirradiation. In addition, we observed a decrease in the PL intensity and lifetime by UV irradiation after Vis irradiation, which is attributed to an increase in  $E$  between **QD-Azo** due to increasing spectral overlap by forming *cis*-isomers on the **QDs** (Figure S13). The TEM images of the UV-Vis irradiated coaggregates (referred to as (**Agg<sub>QD-Azo</sub>**)<sup>UV-Vis</sup>) showed dispersed **QDs** and small coaggregates without the high-order **QD** arrangement (Figure 6c, Figure S14). Thus, we concluded that the increase in the PL intensity is induced by the deformation of the arranged **QD** structure.

To further investigate the effect of photoirradiation, we carried out continuous irradiation only with a UV lamp (referred to as (**Agg<sub>QD-Azo</sub>**)<sup>UV</sup>). As a result, the PL intensity increased gradually upon irradiation, suggesting a decrease in  $E_{QD-QD}$  (Figure 6d). The PL decay

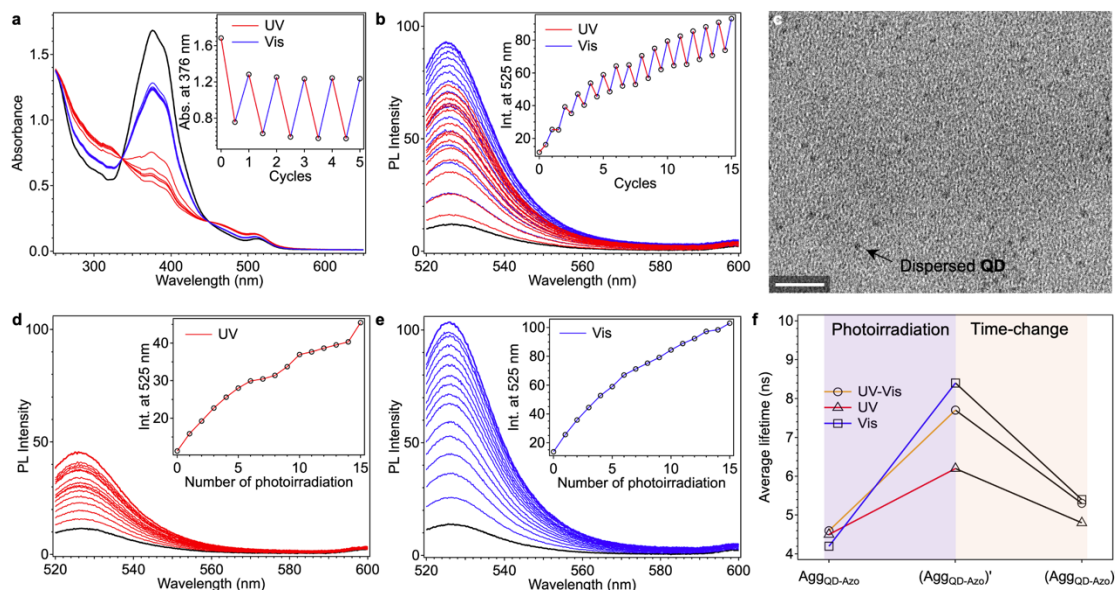


**Figure 6.** (a,b) Changes in the absorption (a) and PL spectra (b) of  $\text{Agg}_{\text{QD-Azo}}$  by repetitious photoirradiation with UV and visible lamps. (c) TEM image of the UV-Vis irradiated  $(\text{Agg}_{\text{QD-Azo}})_{\text{UV-Vis}}$ . The scale bar is 20 nm. (d,e) Changes in the PL spectra of  $\text{Agg}_{\text{QD-Azo}}$  by continuous photoirradiation with UV and visible lamps. (f) Plots of the average lifetime against  $\text{Agg}_{\text{QD-Azo}}$  and photoirradiated  $(\text{Agg}_{\text{QD-Azo}})'$  and time-aged  $(\text{Agg}_{\text{QD-Azo}})''$ .

curves showed an increase in  $\tau_{\text{ave}}$  from 4.5 to 6.2 ns, by which the  $E$  value decreased from 0.79 to 0.71 (Figure S12b, Table S3). As mentioned above, the  $E_{\text{QD-Azo}}$  should increase by the formation of *cis*-isomers. Therefore, the change in  $E_{\text{QD-QD}}$  by photoirradiation is larger than that in  $E_{\text{QD-Azo}}$ . Similarly, upon continuous irradiation with only the Vis lamp (referred to as  $(\text{Agg}_{\text{QD-Azo}})_{\text{Vis}}$ ), a PL increase was observed (Figure 6e). The PL decay curves showed an increase in  $\tau_{\text{ave}}$  from 4.2 to 8.4 ns, by which the  $E$  value decreased from 0.80 to 0.61 (Figure S12c, Table S4). Compared to the results of continuous UV irradiation, the degree of the PL increase was high. This result is due to a low percentage of *cis*-isomers (ca. 20%) because the excitation wavelength at 470 nm is unfavourable for the formation of *cis*-isomers (Figure S15). Given that the PL enhancement was also observed by Vis irradiation even in the presence of a few *cis*-isomers, the photoirradiation-induced PL enhancement is presumably independent of the fraction of *cis*-isomers. Under photoirradiation, generally, isomerization between *trans*- and *cis*-isomers continuously occurs.<sup>[27] [47]</sup> The continuous isomerization via the large structural change between the isomers on the QDs can facilitate the motion of Azo molecules in the coaggregates, leading to the deformation of the  $\text{Agg}_{\text{QD-Azo}}$  into  $(\text{Agg}_{\text{QD-Azo}})'$  without the high-order QD arrangement. Considering these facts, the frequency of photoisomerization rather than the percentage of *cis*-isomers plays an important role in deforming the highly ordered  $\text{Agg}_{\text{QD-Azo}}$ , which leads to a PL enhancement.

The photoirradiated  $(\text{Agg}_{\text{QD-Azo}})'$  is kinetically formed by continuous photoirradiation. Therefore,  $(\text{Agg}_{\text{QD-Azo}})'$  is expected to further change to thermodynamically stable coaggregates. Indeed, the photoirradiated  $(\text{Agg}_{\text{QD-Azo}})_{\text{UV-Vis}}$  underwent a decrease in the PL intensity and lifetime after one day in dark to be time-aged coaggregates (referred to as  $(\text{Agg}_{\text{QD-Azo}})''$ ) (Figure S12, 16a–c). The  $\tau_{\text{ave}}$  value changed to approximately 5 ns, which is similar to that of intact  $\text{Agg}_{\text{QD-Azo}}$  (4.5 ns) (Figure 6f, Tables S2–4). This result indicates that the  $\text{FRET}_{\text{QD-QD}}$  was recovered as a result of the rearrangement of QDs over time. The recovery of rearranged QDs was confirmed by TEM, but

the multilayer structures were not formed (Figure S16d). The reason why the multilayer was not reconstructed by time-aging of  $(\text{Agg}_{\text{QD-Azo}})_{\text{UV-Vis}}$  is probably that after photoirradiation the smaller Azo aggregates compared to  $\text{Agg}_{\text{Azo}}$  are formed and then adsorbed to QDs, which cannot lead to the formation of the highly ordered multilayer. This result suggests that the multilayers could be formed only by mixing the 2D aggregates of Azo ( $\text{Agg}_{\text{Azo}}$ ) and QDs. Based on the results, we concluded that the nanosheets with QD arrangements was recovered by time, while the further organized multilayer structures cannot be reconstructed. Also, the time-changes of photoirradiated  $(\text{Agg}_{\text{QD-Azo}})_{\text{UV}}$  and  $(\text{Agg}_{\text{QD-Azo}})_{\text{Vis}}$  were observed by PL and lifetime measurements (Figure S12, 16), suggesting the similar recovery of the  $\text{FRET}_{\text{QD-QD}}$ .

In addition, we investigated the relationship between the decrease of *cis*-isomers and PL decrease by time-dependent absorption and PL spectra of  $(\text{Agg}_{\text{QD-Azo}})_{\text{Vis}}$  (Figure S17). After 15 min in dark, the *cis*-to-*trans* isomerization through thermally induced isomerization was almost completed. In contrast, the PL decrease was gradually occurred over several hours, suggesting the slow recovery of  $\text{FRET}_{\text{QD-QD}}$ . Accordingly, we could succeed in the reversible control of the QD–QD interaction for the first time.

## Conclusion

In conclusion, we have succeeded in the formation of highly ordered quantum dot supramolecular coaggregates by using the self-assembled azobenzene molecules. Furthermore, continuous photoisomerization enables PL enhancement by controlling the energy transfer efficiency between arranged quantum dots. After one day in dark, the coaggregates exhibiting energy transfer can recover, as supported by thermal back-isomerization. These results demonstrate a novel rational strategy in which the use of self-assembling molecules enables the creation of highly ordered nanoparticle materials. In addition,

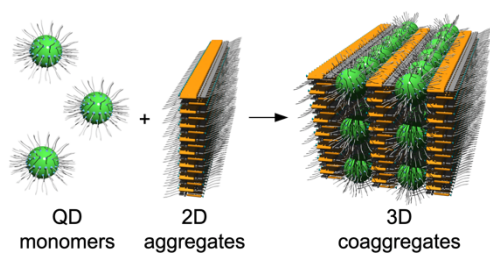
the established methodology for photoresponsive quantum dot materials can lead to new stimuli-responsive materials involving nanoparticles.

## Acknowledgements

This work was supported by Grants-in-Aid for Scientific Research (Nos. 18H01958, 18K14195) from the Japan Society for the Promotion of Science (JSPS). TEM measurement was partially supported by Prof. Dr. K. Kamada and Dr. T. Uchida at National Institute of Advanced Industrial Science and Technology (AIST). The DLS measurements were partially supported by Prof. Dr. S. Yagai at Chiba University.

**Keywords:** self-assembly • azobenzene • quantum dot • photoisomerization • supramolecular chemistry

- [1] H. Wu, M. Fuxreiter, *Cell* **2016**, *165*, 1055-1066.
- [2] D. M. Raymond, B. L. Nilsson, *Chem. Soc. Rev.* **2018**, *47*, 3659-3720.
- [3] S. P. W. Wijnands, E. W. Meijer, M. Merkx, *Bioconjug Chem* **2019**, *30*, 1905-1914.
- [4] A. Wu, L. Isaacs, *J. Am. Chem. Soc.* **2003**, *125*, 4831-4835.
- [5] M. M. Safont-Sempere, G. Fernandez, F. Wurthner, *Chem. Rev.* **2011**, *111*, 5784-5814.
- [6] M. J. Mayoral, C. Rest, J. Schellheimer, V. Stepanenko, G. Fernandez, *Chem. Eur. J.* **2012**, *18*, 15607-15611.
- [7] D. Gori, X. Zhang, V. Stepanenko, F. Wurthner, *Nat. Commun.* **2015**, *6*, 7009.
- [8] Y. S. Wang, T. Feng, Y. Y. Wang, F. E. Hahn, Y. F. Han, *Angew. Chem. Int. Ed.* **2018**, *57*, 15767-15771.
- [9] K. Aratsu, R. Takeya, B. R. Pauw, M. J. Hollamby, Y. Kitamoto, N. Shimizu, H. Takagi, R. Haruki, S. I. Adachi, S. Yagai, *Nat. Commun.* **2020**, *11*, 1623.
- [10] A. Sarkar, T. Behera, R. Sasmal, R. Capelli, C. Empereur-Mot, J. Mahato, S. S. Agasti, G. M. Pavan, A. Chowdhury, S. J. George, *J. Am. Chem. Soc.* **2020**, *142*, 11528-11539.
- [11] A. P. Alivisatos, *Science* **1996**, *271*, 933-937.
- [12] aD. V. Talapin, J. S. Lee, M. V. Kovalenko, E. V. Shevchenko, *Chem. Rev.* **2010**, *110*, 389-458; bW. R. Algar, K. Susumu, J. B. Delehanty, I. L. Medintz, *Anal. Chem.* **2011**, *83*, 8826-8837.
- [13] M. K. Choi, J. Yang, T. Hyeon, D.-H. Kim, *npj Flexible Electronics* **2018**, *2*, 10.
- [14] L. Protesescu, S. Yakunin, M. I. Bodnarchuk, F. Krieg, R. Caputo, C. H. Hendon, R. X. Yang, A. Walsh, M. V. Kovalenko, *Nano Lett.* **2015**, *15*, 3692-3696.
- [15] F. Purcell-Milton, A. K. Vishratina, V. A. Kuznetsova, A. Ryan, A. O. Orlova, Y. K. Gun'ko, *ACS Nano* **2017**, *11*, 9207-9214.
- [16] B. Fisher, J. M. Caruge, D. Zehnder, M. Bawendi, *Phys. Rev. Lett.* **2005**, *94*, 087403.
- [17] B. Mahler, P. Spinicelli, S. Buil, X. Quelin, J. P. Hermier, B. Dubertret, *Nat. Mater.* **2008**, *7*, 659-664.
- [18] H. Takata, H. Naiki, L. Wang, H. Fujiwara, K. Sasaki, N. Tamai, S. Masuo, *Nano Lett.* **2016**, *16*, 5770-5778.
- [19] H. Yoshimura, M. Yamauchi, S. Masuo, *J. Phys. Chem. Lett.* **2020**, *11*, 530-535.
- [20] C. Giansante, L. Carbone, C. Giannini, D. Altamura, Z. Ameer, G. Maruccio, A. Loiudice, M. R. Belviso, P. D. Cozzoli, A. Rizzo, G. Gigli, *J. Phys. Chem. C* **2013**, *117*, 13305-13317.
- [21] N. Kholmicheva, N. Razgoniaeva, P. Yadav, A. Lahey, C. Erickson, P. Moroz, D. Gamelin, M. Zamkov, *J. Phys. Chem. C* **2017**, *121*, 1477-1487.
- [22] M. Matsubara, W. Stevenson, J. Yabuki, X. Zeng, H. Dong, K. Kojima, S. F. Chichibu, K. Tamada, A. Muramatsu, G. Ungar, K. Kanie, *Chem* **2017**, *2*, 860-876.
- [23] C. Zhou, Y. Zhong, H. Dong, W. Zheng, J. Tan, Q. Jie, A. Pan, L. Zhang, W. Xie, *Nat. Commun.* **2020**, *11*, 329.
- [24] M. Yamauchi, S. Masuo, *Chem. Eur. J.* **2020**, *26*, 7176-7184.
- [25] M. Yamauchi, S. Masuo, *Chem.-Eur. J.* **2019**, *25*, 167-172.
- [26] T. Fujino, S. Y. Arzhantsev, T. Tahara, *J. Phys. Chem. A* **2001**, *105*, 8123-8129.
- [27] H. M. Bandara, S. C. Burdette, *Chem. Soc. Rev.* **2012**, *41*, 1809-1825.
- [28] J. Jasieniak, L. Smith, J. van Embden, P. Mulvaney, M. Califano, *Journal of Physical Chemistry C* **2009**, *113*, 19468-19474.
- [29] L. Zang, Y. Che, J. S. Moore, *Acc. Chem. Res.* **2008**, *41*, 1596-1608.
- [30] P. A. Korevaar, C. Schaefer, T. F. de Greef, E. W. Meijer, *J. Am. Chem. Soc.* **2012**, *134*, 13482-13491.
- [31] C. Kulkarni, K. K. Bejagam, S. P. Senanayak, K. S. Narayan, S. Balasubramanian, S. J. George, *J. Am. Chem. Soc.* **2015**, *137*, 3924-3932.
- [32] T. Ren, P. K. Mandal, W. Erker, Z. Liu, Y. Avlasevich, L. Puhl, K. Mullen, T. Basche, *J. Am. Chem. Soc.* **2008**, *130*, 17242-17243.
- [33] E. R. Goldman, I. L. Medintz, J. L. Whitley, A. Hayhurst, A. R. Clapp, H. T. Uyeda, J. R. Deschamps, M. E. Lassman, H. Mattoussi, *J. Am. Chem. Soc.* **2005**, *127*, 6744-6751.
- [34] N. Kholmicheva, P. Moroz, H. Eckard, G. Jensen, M. Zamkov, *ACS Energy Letters* **2016**, *2*, 154-160.
- [35] K. Tvrdy, P. A. Frantsuzov, P. V. Kamat, *Proc Natl Acad Sci U S A* **2011**, *108*, 29-34.
- [36] J. Lakowicz, *Springer, New York* **2006**, XXVI, 954.
- [37] L. Zhu, M. Q. Zhu, J. K. Hurst, A. D. Li, *J. Am. Chem. Soc.* **2005**, *127*, 8968-8970.
- [38] J. B. Hoffman, H. Choi, P. V. Kamat, *J. Phys. Chem. C* **2014**, *118*, 18453-18461.
- [39] K. Boeneman, D. E. Prasuhn, J. B. Blanco-Canosa, P. E. Dawson, J. S. Melinger, M. Ancona, M. H. Stewart, K. Susumu, A. Huston, I. L. Medintz, *J. Am. Chem. Soc.* **2010**, *132*, 18177-18190.
- [40] S. Yagai, T. Karatsu, A. Kitamura, *Chem. Eur. J.* **2005**, *11*, 4054-4063.
- [41] N. Hosono, T. Kajitani, T. Fukushima, K. Ito, S. Sasaki, M. Takata, T. Aida, *Science* **2010**, *330*, 808-811.
- [42] A. Gopal, M. Hifsudheen, S. Furumi, M. Takeuchi, A. Ajayaghosh, *Angew. Chem. Int. Ed.* **2012**, *51*, 10505-10509.
- [43] S. Yagai, M. Yamauchi, A. Kobayashi, T. Karatsu, A. Kitamura, T. Ohba, Y. Kikkawa, *J. Am. Chem. Soc.* **2012**, *134*, 18205-18208.
- [44] B. Adhikari, Y. Yamada, M. Yamauchi, K. Wakita, X. Lin, K. Aratsu, T. Ohba, T. Karatsu, M. J. Hollamby, N. Shimizu, H. Takagi, R. Haruki, S. I. Adachi, S. Yagai, *Nat. Commun.* **2017**, *8*, 15254.
- [45] M. R. Molla, P. Rangadurai, L. Antony, S. Swaminathan, J. J. de Pablo, S. Thayumanavan, *Nat Chem* **2018**, *10*, 659-666.
- [46] aM. Yamauchi, K. Yokoyama, N. Aratani, H. Yamada, S. Masuo, *Angew. Chem. Int. Ed.* **2019**, *58*, 14173-14178; bK. Yano, Y. Itoh, F. Araoka, G. Watanabe, T. Hikima, T. Aida, *Science* **2019**, *363*, 161-165.
- [47] M. Hada, D. Yamaguchi, T. Ishikawa, T. Sawa, K. Tsuruta, K. Ishikawa, S. Y. Koshihara, Y. Hayashi, T. Kato, *Nat. Commun.* **2019**, *10*, 4159.

**Entry for the Table of Contents*****Highly Ordered Quantum Dot Aggregates***

The highly ordered coaggregates of quantum dots (QDs) with inter-QD interaction can be created by using the self-assembled azobenzene derivatives. Furthermore, the inter-QD interaction can be reversibly controlled by photoirradiation and time-aging.